Corrosion behaviour of cast and deformed copper-carbon nanotube composite wires in chloride media

Pyry-Mikko Hannula[a,*], Nicolas Masquelier[b], Sanni Lassila[a], Jari Aromaa[a], Dawid Janas[c], Olof Forsén[a], Mari Lundström[a]

[a] *Aalto University, Department of Chemical and Metallurgical Engineering, School of Chemical Engineering, Vuorimiehentie 2, 02150 Espoo, Finland*

[b] *Nexans Research Centre Lens, Boulevard du Marais, 62301 Lens, France*

[c] *Department of Chemistry, Silesian University of Technology, B. Krzywoustego 4, 44-100 Gliwice, Poland*

Abstract

Copper-carbon nanotube (Cu-CNT) composite wires were produced by casting, rolling and drawing to produce composites with 0.05 wt% CNTs embedded at the grain boundaries of copper. The corrosion properties of wires were investigated in mild and highly corrosive media: solution I consisting of 0.05 wt% sodium chloride (NaCl) and 0.4 wt% ammonium sulfate $(NH_4)_2SO_4$ and solution II consisting of 3.5 wt% NaCl. Composite samples showed similar behaviour and corrosion rates as oxygen free copper in solution I. In 3.5 wt% NaCl all composite samples showed slight improvement in corrosion resistance when compared with oxygen free copper. The corroded wire surfaces after five days in 3.5 wt% NaCl showed less dissolution for composite samples compared with pure copper. The observed decreased corrosion rate for composite wires with embedded CNTs is suggested to be due to reduced cathodic reaction. Galvanic current density between pure copper and carbon nanotubes was observed by mixed potential theory and zero resistance amperometry, neither of which showed tendency towards microgalvanic activity. The results indicate similar or slightly improved corrosion properties of copper containing small additions of CNTs in chloride containing media.

Keywords: Corrosion; Carbon nanotube; Copper; Composite; Seawater; Wire

* Corresponding author. E-mail address: pyry.hannula@aalto.fi (P.-M. Hannula).

1. Introduction

There is a growing demand to improve electrical conductor materials to achieve lighter, stronger and more conductive mate-rials for electrical transmission in power lines as well as in electronics and electrical wiring. Metal matrix composites (MMC) with embedded carbon nanotubes (CNTs) have been envisioned to replace current conductor materials as intrinsic CNT properties provide unique thermal [1] and electrical [2] conductivity, current carrying capacity [3] and mechanical properties [4] even at low concentrations. Copper-carbon nanotube composites have shown enhanced specific conductivity and resistance to copper electro-migration [5] along with improvements in yield strength [6] and tensile strength [7]. There are a variety of manufacturing methods for Cu-CNT composites including casting [8], electrochemical deposition [5,9,10], and powder metallurgy [11] processing routes. While the beneficial electrical and mechanical properties of Cu-CNT composite conductors have been widely studied, the corrosion behaviour of these composites is a novel issue that has not been thoroughly investigated. The operation, lifetime and failure of conductors is strongly affected by their corrosion behaviour and dictates the possible future applications. Therefore, the corrosion behaviour of these composites is of great importance.

Copper and its alloys have excellent corrosion resistance and as such are used extensively in corrosive environments such as seawater. In general, the factors affecting the corrosion of composite materials are well known. Microgalvanic corrosion is known to be an issue for such materials due to the galvanic coupling of the different materials in electrical contact in the composite. Carbon nanotubes and copper do not react with one another to form compounds as they are insoluble and are connected only with a mechanical bond. It is well known that copper will act as the anode and carbon material as the cathode as carbon is more noble in the galvanic series of metals. Corrosion of copper MMC reinforced with stainless steel has been studied in chloride media and it was found that copper will act as the anode and therefore corrode [12]. In

the case of metal-CNT composites some results have been reported for electrochemically produced Ni-CNT coatings, which suggest improved corrosion resistance compared to pure Ni [13-15].Enhanced corrosion properties have also been shown for copper structures with graphene [16] and carbon nanotube [17] coatings, with the increase in corrosion resistance related to the quality and continuity of the coating. The corrosion behaviour of copper-CNT micropillars by electrodeposition has been investigated in chloride media and it was found that the corrosion resistance was improved by an order of magnitude compared to pure copper [18]. In contrast, copper-graphite MMCs have shown conflicting corrosion behaviour in chloride media: both increased corrosion resistance (increasing with graphite content) [19] and decreased corrosion resistance (decreasing with graphite content) [20]. As such, the corrosion behaviour of novel Cu-CNT composite wires in chloride media likely depends on the employed processing technique and resulting microstructure and warrants more comprehensive studies.

The aim of the present communication was to explore the corrosion properties of copper wires with embedded carbon nanotubes in two different chloride media. These composites were prepared by casting, rolling and drawing in dimensions typical for standard copper conductor wires as a novel alternative to commercial copper wire conductors.

2. Experimental

2.1. Preparation of the composite wires

Four different Cu-CNT composite wires were produced by casting for corrosion studies, designated as samples A, B, C and D. All composite wires had similar content of 0.05 wt% embedded CNTs. An industrial grade oxygen free copper wire (Aurubis, Belgium) designated as CuOF was used as the reference material. In order to prepare the wire samples, oxygen free copper was melted by induction at 1300°C. To effectively embed carbon nanotubes inside a copper matrix by casting, the following procedure was applied: First, a thin layer of CNTs (ca.10 μm) was coated onto an oxygen free copper wire, with the method reported previously

[21]. This CNT coated copper wire was then electrodeposited copper from typical copper sulfate electrolyte to produce a sandwich Cu-CNT-Cu wire that could be easily manipulated. This wire was introduced into liquid copper during casting by using a hollow casting pin. The sandwich structure prevents CNT agglomeration and CNTs disperse easily in liquid copper. Due to the casting pin the sandwich Cu-CNT-Cu wire can be introduced close to the copper solidification area thus ensuring homogeneous distribution of CNTs in copper. Due to this procedure, the CNTs are not thermodynamically separated from the copper and are trapped at the grain boundaries during solidification. CNTs consisted of multiwalled tubes with outer diameter 30-40 nm and length of 10 μm (provided by University of Cambridge, UK). Wire rods 15 mm in diameter were cast at a speed of approximately 6 kg/h. After casting the rod samples were transformed to final shape: Sample A was rolled to 3.3 mm in diameter and then cold drawn to 1 mm diameter wire, samples Band C were deformed by rolling to 11 mm in diameter and then cold drawn to 1 mm diameter wire and sample D was rolled to 11 mm diameter and then cold drawn to 0.4 mm wire. Samples A and B were from the same cast but with different diameter after rolling. CuOF reference sample was produced from industrial grade oxygen free copper that was rolled and drawn to 1 mm from original 12 mm diameter rod.

For microstructural observation of wire cross-sections the wires were prepared as such: First, the wires were cast in epoxy. Then, the wire surface was mechanically polished by grinding gradually from 80 to 1200 with silicon carbide grinding paper. Then, the surface was finely polished using silicon carbide preparation with particle sizes 3mm and 1mm. Finally, an oxide polishing solution of 20 nm alumina oxide particles was applied during circa 1 min to obtain a mirror surface. The surface was then cleaned in deionized water and isopropanol alcohol. Finally, the surface was etched chemically for ca. 1 min by a solution of 50 ml of ethanol, 10 ml hydrochloric acid and 5 g ferric chloride. Before electrochemical testing, all samples were cleaned in ethanol under ultrasonication (Elma S15h, Germany) for 15 min and rinsed with DI-water.

2.2. Corrosion testing

Corrosion testing of the composite samples consisted of electrochemical measurements including polarization curve measurement, long-term free corrosion potential (FCP), linear polarization resistance (LPR) measurement and zero resistance amperometry (ZRA). In addition, weight loss testing was conducted for the samples. These tests were performed in two typical corrosive mediums if not otherwise stated, i.e. solution I (0.05 wt% sodium chloride (NaCl) and 0.4 wt% ammonium sulfate ($(NH_4)_2SO_4$)), which is a relatively mild corrosive medium typically used in prohesion testing (ASTM G85 A5) and solution II (3.5 wt% sodium chloride solution), which is commonly used to observe accelerated corrosion mechanisms [22]. Solution I simulates typical corrosive composition of rain water of a coastal industrial location while solution II is similar to marine environments. All electrochemical experiments were conducted with a potentiostat (Gill AC, ACM Instruments, UK) controlled by a personal computer using ACM Sequencer software. The cell was a decanter glass with 300 ml volume.

The polarization measurements were carried out in a three-electrode cell at room temperature without stirring. The reference electrode was a standard calomel electrode (Schott AG, Germany), and platinum (approximate area 10 cm^2) was used as the auxiliary electrode. The used wire samples were 3 cm long and acted as the working electrode. The potential was let to stabilize in the test solution for 10 min before beginning the experiment. During measurements, the current density was measured as a function of the potential between -200 and 500 mV vs. corrosion potential for 35 min, sweep rate being 20 mV/min. The distance between the working and auxiliary electrode was 2.5 cm. Tafel extrapolation method was used to estimate corrosion rate and slopes from polarization curves. We extrapolated the linear anodic and cathodic slopes to the corrosion potential and chose the average of the intersection values as the corrosion current density. The linear range of anodic and cathodic branches was identified for all samples from between 100 and 200 mV from E_{corr} and was averaged from three measurements. The free corrosion potential (FCP) variations of the samples were monitored in both solutions for 30 h.

Linear polarization resistance (LPR) is a non-destructive method, which does not influence the samples. This method was used to estimate the corrosion current density, i_{corr}, for extended periods of time (>35 h). These measurements were conducted with a three-electrode cell similar to the polarization tests. For working electrodes, 4 cm long pieces of wire samples were cut. The tests were initiated as soon as the electrode under investigation was placed in the solution. The vessel was covered with a laboratory film to prevent evaporation but with a few small holes to supply oxygen. The LPR test was set to measure linear polarization resistance every 30 min, the polarization sweep being between 10 mV below and above the rest potential. Used sweep rate was 10 mV/min. The distance between the working and auxiliary electrode was 2.5 cm. The tests were conducted until the observed LPR values were stable. The LPR values were used to calculate the corrosion current density of each sample from the anodic and cathodic slopes obtained from Tafel analysis.

Zero resistance amperometry measurements were also carried out to probe the galvanic interaction in Cu-CNT composites. In these experiments, a commercial grade copper sheet of 99.99% purity (working electrode) was connected to an auxiliary electrode of either a planar carbon nanotube film formed of multiwall carbon nanotubes [23]. The CNT film and copper sheet were fixed at a distance of 5 cm with both electrodes having the same surface area (approximately 5 cm2) and the potential difference between the electrodes set to zero. The resulting current passing through the electrodes was then recorded. Experiments were repeated at least twice in both electrolytes.

Weight loss experiments were carried out during 6 weeks by using a planned interval corrosion test using standard ASTM G31-72 [22] in solution I. Samples consisted of 3 cm long wires with1 mm diameter. Samples were weighed with a scale (AT261 Delta Range, Mettler Toledo, USA) with an accuracy of 10 mg before and after immersion. Tests were carried out in two sealed glass cells in solution I to investigate weight loss after different periods of time. The solution exposed to sample surfaces was adjusted to 30 ml/cm^2, in accordance with the standard

and the samples were fixed so that all wires were equally and fully exposed in the solution. Corrosion product layers were removed by quickly dipping in 5 wt%HNO3solution and ultrasonicated in ethanol for 30 min to produce a surface free of passivation layers. These samples were then imaged by LEO 1450 VP scanning electron microscope (SEM).

Wire samples were cast in epoxy and polished with 1mm diamond paste to expose smooth cross-sections. These samples were then immersed in 3.5 wt% NaCl (solution II) for 5 days to initiate the corrosion process. The corrosion product layer was then removed by ultrasonication in ethanol for 30 min before imaging. SEM im-aging was carried out with Nanolab 600 Dual Focused Beam System (FEI HELIOS). ImageJ software was used to analyze the corroded wire samples from SEM images. The analysis was conducted from multiple locations along each wire cross-section, representing the typical surface

3. Results and discussion

3.1. Microstructure of the experimental materials

Typical Cu-CNT composite sample microstructure is shown in Fig. 1. In all composite samples, most of the CNTs were found clustered at and nearby the grain boundaries while some CNTs could also be seen also inside the grains. Fig. 1a shows the typical composite microstructure after etching. The image shows nearly the whole cross-section of sample D. No porosity could be observed on the samples. The grain boundaries are clearly covered in CNTs. This is attributed to the insolubility of CNTs with Cu, which forces CNTs to segregate at the grain boundaries of copper as it solidifies. Fig. 1b shows a close-up of a CNT cluster at the grain boundary. In Fig. 1c individual CNTs can be seen sticking out of the grain boundary. No observable porosity could be seen from the samples.

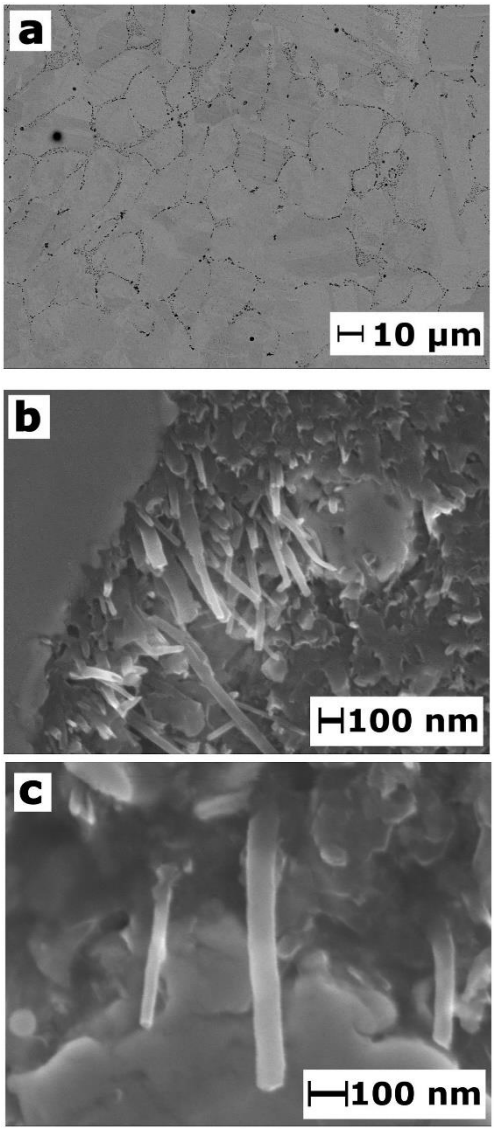

Fig. 1 Typical Cu-CNT composite microstructure by SEM (a) after chemical etching(sample C), (b) showing CNT cluster at grain boundary (sample D) and (c) showing individual CNTs sticking out from Cu matrix (sample D).

3.2. Polarization behaviour and corrosion rate

Figs. 2 and 3 show the polarization curves of Cu-CNT wires (A-D) and CuOF wire investigated in solution I and solution II. Clearly, the CNTs have no significant effect on the anodic polarization of the wires in mildly corrosive solution I with all samples showing similar anodic features and corrosion potential, Fig. 2. Samples A-C also showed slightly lower cathodic Tafel slope.

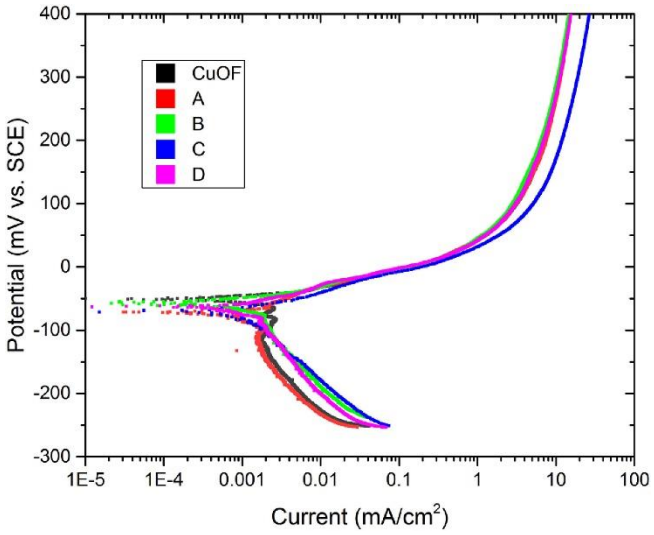

Fig. 2 Polarization curves of CuOF and Cu-CNT samples A-D in solution I consisting of 0.05 wt% sodium chloride (NaCl) and 0.4 wt% ammonium sulfate ($(NH_4)_2SO_4$).

In solution II (3.5 wt% NaCl) all samples exhibited similar corrosion potential, but the cathodic polarization behaviour was not identical. All composite samples and oxygen free copper showed a clear peak at -30...-10 mV vs. SCE in 3.5 wt% NaCl, which is attributed to the formation of copper chloride film [24,25]. The three typically proposed mechanisms in literature for the formation of the CuCl film are [25]

$$Cu + 2Cl^- \leftrightarrow CuCl_2^- + e^- \quad (1)$$

or

$$Cu \leftrightarrow Cu^+ + e^- \quad (2)$$

$$Cu^+ + 2Cl^- \leftrightarrow CuCl_2^- \quad (3)$$

or

$$Cu + Cl^- \leftrightarrow CuCl + e^- \quad (4)$$

$$CuCl_2^- \leftrightarrow CuCl + Cl^- \quad (5)$$

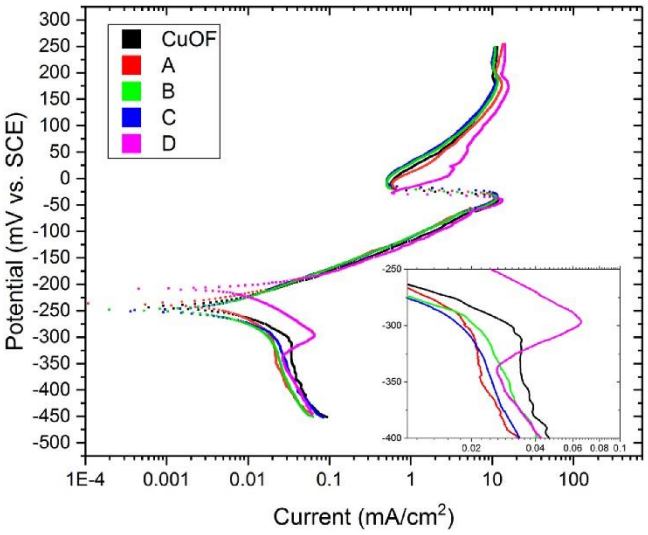

Fig. 3 Polarization curves of CuOF and Cu-CNT samples A-D in solution II (3.5 wt%NaCl), inset of cathodic slope.

In reaction (1) and (4) & (5) the copper directly dissolves to form cuprous chloride species, whereas in (2) & (3) copper is first dissolved as a cuprous ion before forming copper chloride. The cathodic reaction is

$$2H_2O + O_2 + 4e^- \leftrightarrow 4OH^-$$

As the anodic slopes were identical between all samples in same solutions, results have been omitted from Table 1. The anodic slope (59 mV/decade) in 3.5 wt% NaCl was identical to those previously reported in literature for pure copper without passive film [25]. However, the cathodic reaction (6) was clearly decreased in composite samples in 3.5 wt% NaCl (see inset of Fig. 3, where cathodic current of composite samples is decreased). Cathodic Tafel slope values shown in Table 1 are smaller for all composite samples, also contributing to smaller corrosion current. The CNT additions thus decrease the cathodic reaction rate, while having no effect on the anodic behaviour of copper. Previously, similar results were obtained by Kirkland et al. [26] and Raman et al. [27], who showed reduced cathodic reaction rates and cathodic Tafel slopes on copper inhomogenously coated with graphene in chloride media. Corrosion current density of samples was long-term tested in3.5 wt% NaCl (solution II), Fig. 4, as pure copper and composite

wire samples did not show any difference in mild corrosive medium (solution I). All samples show similar behaviour and i_{corr} begins to stabilize after approximately 25-30 h. After this period all composite samples show slightly decreased i_{corr} compared with oxygen free copper. These results are attributed to the CNT additions and conform with the observed rise in free corrosion potential of composite samples, Fig. 7. In the beginning of the test the CNT additions had no effect on the corrosion properties of composite samples as they were not markedly present at the wire surface. After corrosion has proceeded through the wire surface do the CNTs start to affect the corrosion process due to their inert nature by hindering the corrosion paths in the copper matrix. However, due to the small amount of CNTs (0.05 wt%) embedded in the copper matrix this effect is not as significant as e.g. in the case of carbon based coatings. Graphene and CNT coatings on copper typically show a decrease of an order of magnitude in corrosion current in chloride media [16,17], [26,27], a vastly smaller addition of CNTs embedded in the copper matrix was still shown to decrease the corrosion rate by up to 50% (sample D). During planned interval weight loss measurements for 6 weeks in solution I all composite samples showed similar corrosion rate as reference CuOF. Detailed discussion about these results is provided later in section 3.5. Previous results on corrosion of pure copper in 3.5 wt% NaCl show similar corrosion rates ranging from 3.8 $\mu A/cm^2$ [28] to 11.3 $\mu A/cm^2$ [29]. As the CNTs appear to be mostly situated on the grain boundaries of the composite wires, the corrosion rate was related to the grain size of the wire samples. The stable i_{corr} was obtained from Fig. 4and related to the observed grain sizes from cross-sectional images and the results are shown in Fig. 5. Here, it can be observed that the corrosion rate for composite samples in 3.5 wt% NaCl is related to their grain size. As the grain size decreases, the grain boundary area fraction containing CNTs is increased, leading to higher corrosion resistance. The reference CuOF sample does not follow the same trendline. Its corrosion rate (ca. 4.6 $\mu A/cm^2$) is considerably higher than what could be estimated for a composite wire of similar grain size (ca. 3.0 $\mu A/cm^2$). This effect is likely due to

the retardation of the cathodic reaction due to CNT additions, also seen in polarization behaviour (Figs. 3 and 9), which decreases the overall corrosion rate of composite samples.

Table 1. Compiled results from polarization tests, long term corrosion current measurement and weight loss experiments.

Sample	i_{corr} (μA/cm^2) in solution I		i_{corr} (μA/cm^2) in solution II		Cathodic Tafel slopes, β_c (mV/decade)	
	Tafel extrapolation	Weight loss tests after 6 weeks	Tafel extrapolation	After 35 h	Solution I	Solution II
CuOF	1	3.0	11	4.6	147	477
A	1	2.9	8	3.8	133	338
B	1	2.9	7	3.9	130	392
C	1	3.0	8	2.8	108	366
D	1	-	11	2.3	149	308

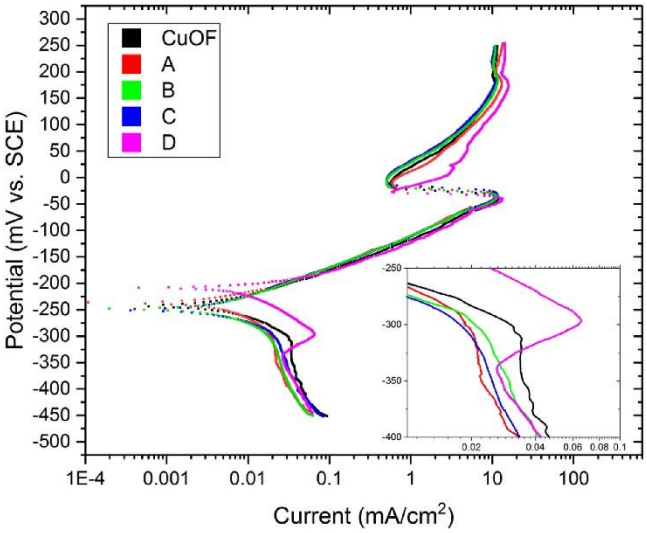

Fig. 4 Corrosion current density recorded every 30 min in solution II (3.5 wt% NaCl) for CuOF and Cu-CNT samples A-D.

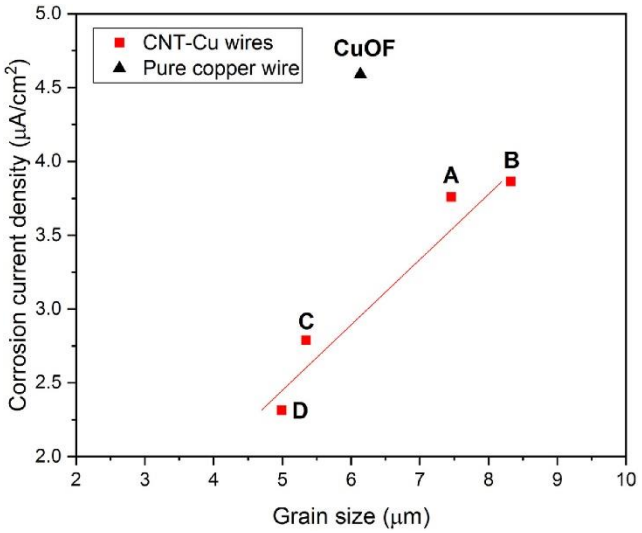

Fig. 5 The correlation between grain size and corrosion current density of CNT-Cu composite wires and reference copper wire.

3.3. Stabilization of free corrosion potential

The variation of free corrosion potential (FCP) with time was also measured for CuOF and samples A-C in both solutions, Fig. 6, Fig. 7. It was found that after 30 h of immersion all FCP values were stable within 215 ± 7 mV vs. SCE in 3.5 wt% NaCl and −35 mV ± 5 mV vs. SCE in solution I. No notable difference between composite samples and CuOF existed in solution I. However, in 3.5 wt% NaCl all measured Cu-CNT samples (A-D) showed slightly more noble FCP values after approximately 17 h. Samples A-D stabilized between −216 mV and −208 mV whereas CuOF stabilized at −221 mV vs. SCE at t = 30 h. The rise in FCP for pure copper is attributed to improvements in passivity by Cu2O layer formation [25,30]. Here, the observed increased rise in passivity is also attributed to the substantially higher nobility of CNTs with respect to copper (see Fig. 7).

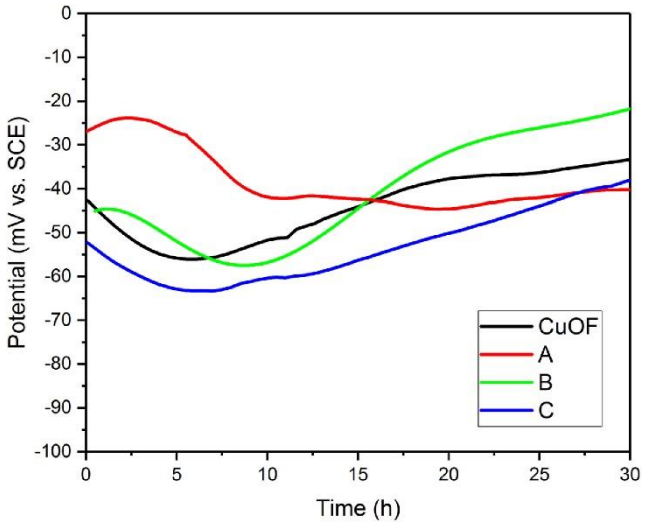

Fig. 6 Free corrosion potential variation with time for samples CuOF and Cu-CNT samples A-C in solution I.

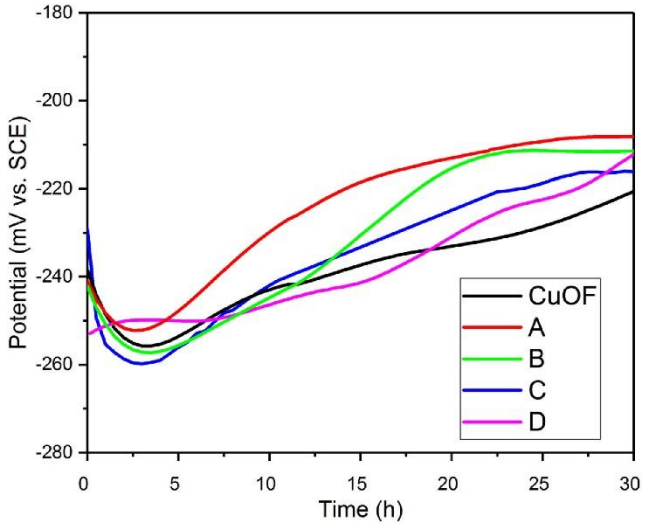

Fig. 7 Free corrosion potential variation with time for samples CuOF and Cu-CNT samples A-D in solution II.

3.4. Weight loss test

Weight loss tests were carried out for samples CuOF and composite samples A, B and C by a planned interval corrosion test in solution I. Table 2 shows the test procedure for weight loss tests according to ASTM G31-72. The test is divided so that each wire is tested for 4 different immersion times. This allows the metal corrosion rate to be compared at different intervals, such as during the first 2 weeks (X1), the last 2 weeks (Y) or during the whole 6 test week period (X_t+1).

Table 2. Planned interval corrosion test for CuOF and composite samples A-C according to ASTM G31-72.

Test specimen sets	X_t+1		
	X_t		Y
	X_1		
Immersion time from beginning of test (weeks)	2	4	6

Table 3 shows the corrosion rate based on measured weight loss. Composite samples A and C were shown to corrode at the same rate as the oxygen free reference sample. Only sample B corroded slightly faster than the other samples. The explanation for increased corrosion of sample B has been described later by microstructural analysis. The corrosion rate of all samples decreased with time.

Table 3. Weight loss of Cu-CNT samples (A-C) and oxygen free copper wire (CuOF) based on planned interval corrosion tests (ASTM G31-72) in solution I.

Sample	Immersion time	Weight loss ($\mu g/cm^2/day$)	i_{corr} ($\mu A/cm^2$)	Thinning ($\mu m/year$)
CuOF	X_t+1	85.1	3.0	34.9
	X_t	94.8	3.4	38.9
	X_1	108.7	3.8	44.6
	Y	121.4	4.3	49.8
A	X_t+1	83.1	2.9	34.1
	X_t	84.2	3.0	34.5
	X_1	112.6	4.0	46.2
	Y	122.8	4.3	50.4
B	X_t+1	108.9	3.9	44.7
	X_t	109.1	3.9	44.7
	X_1	123.7	4.4	50.7
	Y	131.6	4.7	54.0
C	X_t+1	84.9	3.0	34.8
	X_t	103.3	3.7	42.4
	X_1	120.2	4.3	49.3
	Y	123.7	4.3	50.3

Comparing the measured weight loss and Tafel extrapolated corrosion currents in solution I in Table 1, it can be seen that the actual corrosion rate during 6 weeks was about three times higher than what was predicted by Tafel method. This reflects the nature of the polarization measurements, which give the temporary rate of corrosion, but not an exact prediction of long-term behaviour. The observed corrosion rates in solution I were on par with oxygen free copper indicating that the Cu-CNT wires behave similarly as pure copper in mildly corrosive solutions.

3.5. Galvanic current

3.5.1. Zero resistance amperometry

Galvanic current density was measured by the zero resistance amperometry (ZRA) technique in both solutions with equal sized electrodes. Results of ZRA measurements are shown in Fig. 8, where the galvanic current between CNT film and commercial grade oxygen free copper are shown plotted against time up to 50 h. The galvanic current was shown to be in the range of 2–7 $\mu A/cm^2$. The galvanic current density in solution I is larger than observed by Tafel extrapolation in the same solution and similar to results from weight loss measurements. In solution II the observed galvanic current density is smaller than from Tafel extrapolation. The results indicate no substantial microgalvanic activity between the copper matrix and CNT constituent nor does it seem to protect from further corrosion. In ZRA tests the surface areas of copper and CNT were equal, whereas in a composite the area of CNT facing electrolyte will be magnitudes smaller than that of copper, due to the small wt% of CNTs, which will even further reduce the risk of galvanic corrosion. Because of the positive current (CNT material acts as cathode and pure copper as anode) the CNT material is thus more noble and the copper corrodes, albeit slowly.

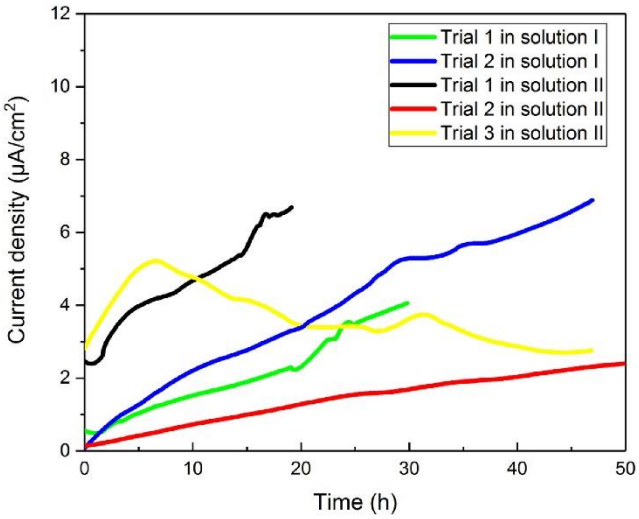

Fig. 8 Variation of galvanic current density between pure copper sheet and carbon nanotube film as a function of time in both solutions.

3.5.2. Mixed potential theory analysis

The galvanic current was also estimated by mixed potential theory, which predicts the galvanic current density of a composite material from the constituents polarization curves. The galvanic current density can be estimated from the intersection point of the cathodic polarization curve of the nobler constituent (CNTs) and anodic polarization curve of the less noble metal (copper). At this intersection, the total rate of oxidation reaction (on copper) is equal to total rate of reduction reaction (on CNT material). Galvanic corrosion would be expected to occur at the interface between CNTs and copper i.e. at the copper grain boundaries.

Polarization curves were recorded for CNT film and oxygen free copper wire in solution II (3.5 wt% NaCl) and the results are presented in Fig. 9. The results can be interpreted for a composite material with equal surface areas of carbon material and copper. Of course, in our case the CNT area is magnitudes smaller than the surrounding copper matrix, decreasing the possible impact of any galvanic corrosion. The results from mixed potential analysis in Fig. 9 show that the observed galvanic corrosion current density between CNTs and copper is 4 $\mu A/cm^2$, which is in good agreement with the values observed in ZRA measurements. The cathodic and anodic current for carbon nanotube material is magnitudes smaller. It can be

concluded from galvanic current measurements that CNT additions do not reduce the corrosion performance of Cu-CNT composites in terms of galvanic corrosion.

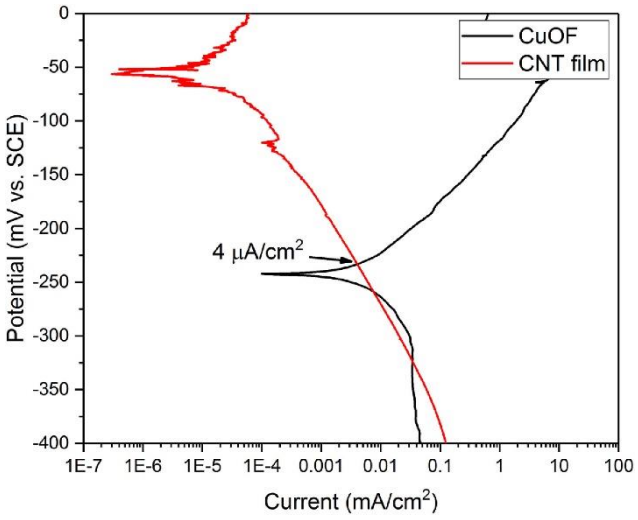

Fig. 9 Polarization curves of oxygen free copper (CuOF) and carbon nanotube (CNT) film in 3.5 wt% NaCl for galvanic current density estimation.

3.6. Microstructural analyses

3.6.1. After immersion in solution I

The surface morphologies of samples were observed before and after weight loss tests in solution I for the exception of sample D, which was not included in the weight loss tests and was only imaged as produced. All samples showed a similar green corrosion product at the wire surface at the end of weight loss testing. The as produced and corroded sample surfaces were cleaned by ultrasonication in ethanol to remove possible grease and corrosion product layers and then observed by SEM once the surface was clean. Fig. 10 (a)-(e) shows the sample microstructures before testing and (a')-(d') after weight loss tests. All samples showed some surface inhomogeneity before corrosion testing; grooves and pits were observed at the wire surface after drawing. However, the largest diameter pits were observed on the surface of sample B.

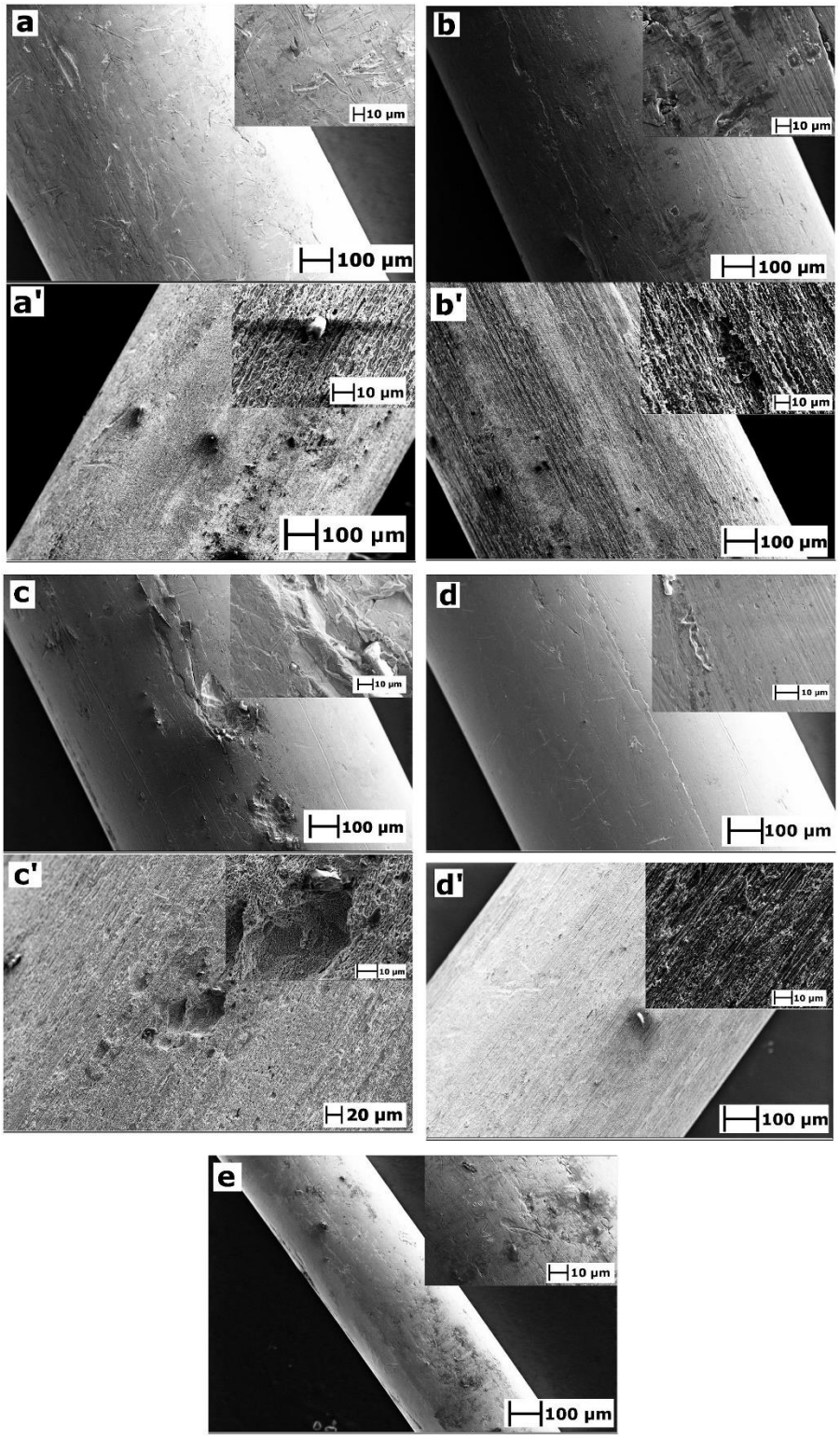

Fig. 20 Samples before and after weight loss test for 6 weeks in solution I (a) CuOF - (a') CuOF after weight loss test, (b) Sample A - (b') Sample A after weight loss test, (c) Sample B - (c') Sample B after weight loss test, (d) Sample C - (d') Sample C after weight loss test, (e) Sample D (not included in weight loss test).

After weight loss testing samples showed signs of general corrosion, as the sample structures were corroded evenly along the axis of the wires. Importantly, no microgalvanic corrosion could be observed as predicted by the ZRA measurements. It is believed that sample B corroded slightly faster than other samples because of the observed high microstructural inhomogeneity at the surface, Fig. 10 (c)-(c'), where pits and grooves on the sample surface are apparent. However, this inhomogeneity is not inherent as other samples did not show similar surfaces.

3.6.2. After immersion in solution II

Fig. 11 shows the microstructure of wires after 5 d immersion in 3.5 wt% NaCl. All samples showed evidence of pitting corrosion. Though the corrosion mechanism did not change, the difference between the corroded microstructure of CuOF and composite samples was evident. In CuOF most of the pits were deep, Fig. 11 a. Next to these deep pits were some shallow pits. The median area of corroded pits in CuOF was 3.4 μm^2. For composite samples the corroded pits were uniformly distributed and typically shallow, with some deeper pits in between. In all composite samples the observed pits were smaller than in CuOF, implying decreased corrosion rates for composite samples. No signs of microgalvanic corrosion on the border of CNT and copper i.e. grain boundaries, could be observed. The corrosion pit median sizes for composite samples were (A) 1.0 μm^2, (B) 3.0 μm^2, (C) 2.0 μm^2 and (D) 1.2 μm^2. The decrease in size of corrosion pits is attributed to the CNT additions, which hinder the corrosion attack by retarding the cathodic reaction when CNTs are exposed to the solution.

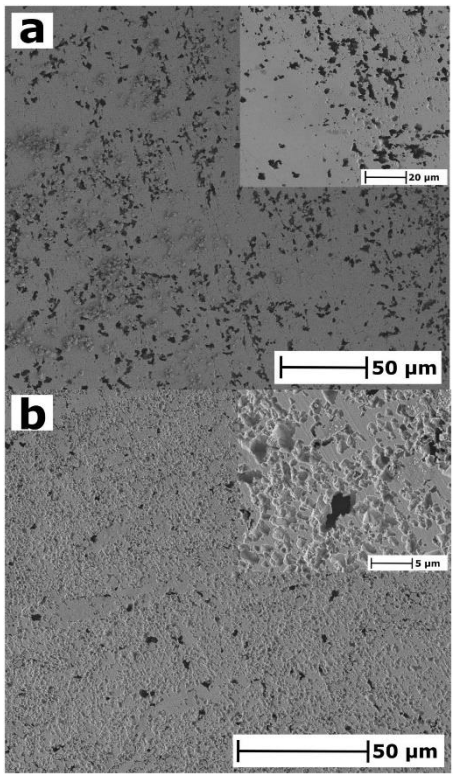

Fig. 31 Microstructure of corroded wire surfaces after 5 days in 3.5 wt% NaCl (a) CuOF and (b) Cu-CNT sample D.

4. Conclusions

The corrosion properties of carbon nanotube-copper composite wires with 0.05 wt% CNTs distributed on the grain boundaries of copper matrix produced by casting, rolling and drawing were measured. Oxygen free copper wire was used as the reference material. The corrosion behaviour of samples were investigated in mild and highly corrosive chloride media. Due to the small concentration of CNTs the observed results showed small, but noticeable changes in corrosion properties. The following conclusions can be derived from the results:

(a) The corrosion properties of composite wire samples were on par with oxygen free copper in mild corrosive media (0.05 wt% sodium chloride (NaCl) and 0.4 wt% ammonium sulfate ($(NH_4)_2SO_4$))). This result is derived from polarization tests, free corrosion potential and weight loss measurements.

(b) Polarization curves of the composite wires showed decreased cathodic reactions in 3.5 wt% NaCl when compared with oxygen free copper. The stabilized corrosion current density ($t \geq 30$ h) of all composite samples from linear polarization resistance measurements was smaller than that of oxygen free copper in 3.5 wt% NaCl. The composite corrosion current density was decreased by up to 50%.

(c) All tested composite samples exhibited higher free corrosion potential than oxygen free copper after 17 h of immersion in 3.5 wt% NaCl. This is in agreement with the lower corrosion current density based on mixed potential theory and due to slower anodic reaction.

(d) Zero resistance amperometry and mixed potential analysis showed no tendency for galvanic corrosion between copper and CNTs and microstructural analysis did not reveal galvanic corrosion taking place on composite samples in either solution.

(e) Addition of CNTs in a copper wire matrix results in a similar or slightly more corrosion resistant material depending on the nature of the employed corrosive media. This study highlights the feasibility of using such composite material in similar or more corrosive settings as typical copper conductor wires.

5. Acknowledgements

This work has been supported by the FP7 European project Ultrawire (Grant Agreement No. 609057). RawMatTERS Finland Infrastructure (RAMI) supported by Academy of Finland is greatly acknowledged. Part of the research was performed at the OtaNano – Micronova Nanofabrication Centre of Aalto University. D.J. thanks National Science Center, Poland (under the Polonez program, grant agreement UMO-2015/19/P/ST5/03799) and the European Union's Horizon 2020 research and innovation programme (Marie Skłodowska-Curie grant agreement 665778). D.J. would also like to acknowledge Foundation for Polish Science for START scholarship.

References

[1] S. Berber, Y. Kwon, D. Tomanek, Unusually high thermal conductivity of carbon nanotubes, Phys. Rev. Lett. 84 (2000) 4613.
[2] H. Li, W. Lu, J. Li, X. Bai, C. Gu, Multichannel ballistic transport in multiwallcarbon nanotubes, Phys. Rev. Lett. 95 (2005), 086601.
[3] B. Wei, R. Vajtai, P. Ajayan, Reliability and current carrying capacity of carbon nanotubes, Appl. Phys. Lett. 79 (2001) 1172.
[4] M.F. Yu, O. Lourie, M.J. Dyer, K. Moloni, T.F. Kelly, R.S. Ruoff, Strength and breaking mechanism of multiwalled carbon nanotubes under tensile load, Science 287 (2000) 637-640.
[5] C. Subramaniam, T. Yamada, K. Kobashi, A. Sekiguchi, D.N. Futaba, M. Yumura, K. Hata, One hundred fold increase in current carrying capacity in a carbon nanotube-copper composite, Nat. Commun. 4 (2013).
[6] K. Kim, J. Eckert, S. Menzel, T. Gemming, S. Hong, Grain refinement assisted strengthening of carbon nanotube reinforced copper matrix nanocomposites, Appl. Phys. Lett. 92 (2008), 121901.
[7] G. Chai, Y. Sun, Q. Chen, Mechanical properties of carbon nanotube copper nanocomposites, J. Micromech. Microeng. 18 (2008), 035013.
[8] P. Kwasniewski, G. Kiesiewicz, Studies on obtaining Cu-CNT composites by continuous casting method, Metallurgy and Foundry Engineering 40 (2014).
[9] P. Hannula, A. Peltonen, J. Aromaa, D. Janas, M. Lundstrom, B.P. Wilson, K. Koziol, O. Forsoen, Carbon nanotube-copper composites by electrodeposition on carbon nanotube fibers, Carbon 107 (2016) 281-287.
[10] P. Hannula, J. Aromaa, B.P. Wilson, D. Janas, K. Koziol, O. Forsoen, M. Lundstrom, Observations of copper deposition on functionalized carbon nanotube films, Electrochim. Acta 232 (2017) 495-504.
[11] W. Chen, J. Tu, L. Wang, H. Gan, Z. Xu, X. Zhang, Tribological application of carbon nanotubes in a metal-based composite coating and composites, Carbon 41 (2003) 215-222.
[12] A. Bakkar, S. Ataya, Corrosion behaviour of stainless steel fibre-reinforced copper metal matrix composite with reference to electrochemical response of its constituents, Corrosion Sci. 85 (2014) 343-351.
[13] X. Chen, C. Chen, H. Xiao, F. Cheng, G. Zhang, G. Yi, Corrosion behavior ofcarbon nanotubeseNi composite coating, Surf. Coating. Technol. 191 (2005)351-356.
[14] S. Khabazian, S. Sanjabi, The effect of multi-walled carbon nanotube pre-treatments on the electrodeposition of NieMWCNTs coatings, Appl. Surf. Sci.257 (2011) 5850-5856.
[15] X. Li, Y. Gu, T. Shi, D. Peng, M. Tang, Q. Zhang, X. Huang, Preparation of the multi-walled carbon nanotubes/nickel composite coating with superior wear and corrosion resistance, J. Mater. Eng. Perform. 24 (2015) 4656-4663.
[16] B.P. Singh, S. Nayak, K.K. Nanda, B.K. Jena, S. Bhattacharjee, L. Besra, The production of a corrosion resistant graphene reinforced composite coating on copper by electrophoretic deposition, Carbon 61 (2013) 47-56.
[17] T. Laoui, Corrosion performance of copper coated with carbon nanotubes, Arabian J. Sci. Eng. 35 (2010) 58.
[18] S. Ghanbari, J. Darabi, Fabrication and material characterization of copper and copper CNT micropillars, Mater. Res. Express 2 (2015), 075501.
[19] H. Zhao, L. Liu, Y. Wu, W. Hu, Investigation on wear and corrosion behavior of Cu graphite composites prepared by electroforming, Compos. Sci. Technol.67 (2007) 1210-1217.
[20] J. Orth, H. Wheat, Corrosion behavior of high energy high rate consolidated graphite/copper metal matrix composites in chloride media, Appl. Compos.Mater. 4 (1997) 305-320.
[21] D. Janas, S.K. Kreft, K.K.K. Koziol, Printing of highly conductive carbon nano-tube fibres from aqueous dispersion, Mater. Des. 116 (2017) 16-20.
[22] J. Aromaa, A. Klarin, Book 15: Materials, Corrosion Prevention and Maintenance, Fapet Oy, Helsinki, 1999, p. 89.
[23] Y.L. Li, I.A. Kinloch, A.H. Windle, Direct spinning of carbon nanotube fibers from chemical vapor deposition synthesis, Science 304 (2004) 276-278.
[24] H. Lee, K. Nobe, Kinetics and mechanisms of Cu electrodissolution in chloride media, J. Electrochem. Soc. 133 (1986) 2035-2043.

[25] G. Kear, B.D. Barker, F.C. Walsh, Electrochemical corrosion of unalloyed copper in chloride media-a critical review, Corrosion Sci. 46 (2004) 109-135.
[26] N. Kirkland, T. Schiller, N. Medhekar, N. Birbilis, Exploring graphene as a corrosion protection barrier, Corrosion Sci. 56 (2012) 1-4.
[27] R.K. Singh Raman, P. Chakraborty Banerjee, D.E. Lobo, H. Gullapalli, M. Sumandasa, A. Kumar, L. Choudhary, R. Tkacz, P.M. Ajayan, M. Majumder, Protecting copper from electrochemical degradation by graphene coating, Carbon 50 (2012) 4040-4045.
[28] E.M. Sherif, A.M. El Shamy, M.M. Ramla, A.O.H. El Nazhawy, 5-(Phenyl)-4H-1,2,4-triazole-3-thiol as a corrosion inhibitor for copper in 3.5% NaCl solutions, Mater. Chem. Phys. 102 (2007) 231-239.
[29] K.F. Khaled, Studies of the corrosion inhibition of copper in sodium chloride solutions using chemical and electrochemical measurements, Mater. Chem.Phys. 125 (2011) 427-433.
[30] ISBN: 0-08170-019-0, A. Handbook, Vol 13: Corrosion: Fundamentals, Testing,and Protection, ASM International, USA, 1987, p. 449.